CHAPTER III

RESULTS

1. Mosquito rearing

1.1 Observation on the life duration, hatchability, pupation and emergence

An iso-female line colony of Thai strain *An. campestris*-like Form E was successfully established under laboratory conditions for more than 40 generations. Detailed life duration of eggs, larvae, pupae, adult females and males of F_1-, F_5-, F_{10}-, F_{20}- and F_{30}-progenies is summarized in Table 1. Observation of the life cycle and developmental period of *An. campestris*-like Form E from the laboratory-raised iso-female line colony (F_1, F_5, F_{10}, F_{20}, F_{30}), demonstrated that the average eggs per deposited female (observation on 20 gravid adult females) were 213.87 ± 96.49 (19-307), 238.17 ± 72.74 (20-296), 201.23 ± 55.03 (57-265), 235.23 ± 59.50 (100-302) and 236.80 ± 71.20 (58-308) in F_1, F_5, F_{10}, F_{20} and F_{30}, respectively. The duration of egg-hatching was 2-4 days, in which the percentage embryonation and hatching was 81-99% and 78-96%, respectively. The larval instars matured in 8-10 days. Pupation duration ranged from 2-3 days, and more than 80% of first instar larvae eventually pupated. More than 85% of pupae successfully emerged as adults.

Table 1 Life duration of *An. campestris*-like Form E from an iso-female line laboratory-raised colony.

Generation	Mean duration in day (range)				
	F_1	F_5	F_{10}	F_{20}	F_{30}
Mosquito stages					
Egg*	2.10 ± 0.30	2.09 ± 0.32	2.09 ± 0.30	2.10 ± 0.32	2.09 ± 0.28
	(2-3)	(2-4)	(2-4)	(2-4)	(2-3)
Larva*	8.71 ± 0.56	7.58 ± 0.57	7.75 ± 0.49	7.79 ± 0.59	9.28 ± 0.62
	(8-10)	(7-9)	(7-9)	(7-9)	(8-10)
Pupa*	2.40 ± 0.50	2.27 ± 0.45	2.37 ± 0.49	2.37 ± 0.49	2.63 ± 0.49
	(2-3)	(2-3)	(2-3)	(2-3)	(2-3)
Adult females**	27.77 ± 9.56	27.13 ± 8.03	27.33 ± 9.57	25.93 ± 8.26	23.33 ± 7.42
	(6-45)	(10-38)	(9-44)	(10-40)	(8-38)
Adult males**	19.67 ± 9.71	16.93 ± 5.63	20.23 ± 9.10	19.73 ± 6.51	17.63 ± 7.08
	(6-39)	(7-30)	(8-38)	(10-35)	(7-34)

* 100 samples for each generation.

** 30 samples for each generation.

1.2 Feeding ability

Results of direct feeding ability on white rat in a 30 x 30 x 30 cm cage, and artificial feeding ability on bovine heparinized-blood in a paper cup (8.5 cm in diameter and 11 cm in depth), of female *An. campestris*-like Form E at different ages ranging from 1 to 10 days, demonstrated that in the cage, adult females aged of 3, 4, 5 and 6 days were successful in feeding on the blood of white rats, with feeding rates of 30%, 39%, 62% and 43%, respectively. Interestingly, the adult females aged 3, 4, 5, and 6 days succeeded in artificial feeding on bovine heparinzed-blood in the paper cup at higher rates than direct feeding on white rat in the cage in all experiments by yielding feeding rates of 62%, 68%, 78% and 61%, respectively (Table 2).

1.3 Ability of free mating in a 30 cm cubed cage

In order to determine the adaptive stenogamy of *An. campestris*-like Form E, the newly emerged females and males co-habitated at a ratio of 150:300, in a 30 x 30 x 30 cm cage for one week. The results indicated that *An. campestris*-like Form E failed to mate freely in the cage at a 0% insemination rate (from experiments repeated 3 times). Additionally, in current studies of various strains, *An. campestris*-like Form B (Kamphaeng Phet: F_{11}) and E (Sa Kaeo: F_{22}, Chanthaburi: F_{11}, Ayutthaya: F_{21}, Maha Sarakham: F_{16}, Udon Thani: F_{11}, Khon Kean: F_{11}, Mukdahan: F_{10}, Prachuap Khiri Khan: F_{10} Chumphon: F_{10}) failed to copulate freely in a 30 x 30 x 30 cm cage as determined by 0% insemination rates, indicating strong eurygamy.

Table 2 Direct feeding ability on white rat in a 30 x 30 x 30 cm cage and artificial feeding ability on bovine heparined blood from different ages of *An. campestris*-like Form E.

Day after emergence	Direct feeding*	Artificial feeding*
	No. successfully fed females (%)	No. successfully fed females (%)
1	13 (13%)	12 (12%)
2	17 (17%)	25 (25%)
3	30 (30%)	62 (62%)
4	39 (39%)	68 (68%)
5	62 (62%)	78 (78%)
6	43 (43%)	61 (61%)
7	24 (24%)	58 (58%)
8	16 (16%)	47 (47%)
9	14 (14%)	48 (48%)
10	12 (12%)	50 (50%)

*100 adult females for each experiment.

1.4 Ability of male in artificial mating

The artificial mating ability of *An. campestris*-like Form E is demonstrated in Table 3. The best age for artificial mating in male was 5-days-old. Nonetheless, males aged 4 to 8 days old could be used satisfactorily.

Table 3 Artificial mating ability of *An. campestris*-like Form E males.

Day after emergence*	No. successfully mated females (%)	No. insemination (%)
1	11 (36.67)	0 (0)
2	23 (76.67)	18 (78.26)
3	23 (76.67)	18 (78.26)
4	30 (100)	24 (80.00)
5	30 (100)	26 (86.67)
6	28 (93.33)	23 (82.14)
7	28 (93.33)	24 (85.71)
8	28 (93.33)	23 (82.14)
9	26 (86.67)	16 (61.54)
10	23 (76.67)	11 (47.83)

*Thirty males for each experiment.

1.5 Ability of eggs deposition

In the case of puting 20 gravid adult females of *An. campestris*-like Form E in a 30 x 30 x 30 cm cage, fewer numbers of eggs were obtained from the oviposition in a plastic cup (9.7 cm in diameter and 11.5 cm in depth), *i.e.*, 0, 0, 279, 0 and 0 eggs per cup were obtained in experiment I (F_5), II (F_{10}), III (F_{15}), IV (F_{20}) and V (F_{30}), respectively. In the case of forced laying of eggs by placing 20 gravid adult females in a plastic cup (2 replicates) in the same size and conditions as used in the cage, a massive number of eggs, *i.e.*, 1,273, 1,318, 1,705, 2,180 and 1,501 eggs per cup, were recovered for experiment I (F_5), II (F_{10}), III (F_{15}), IV (F_{20}) and V (F_{30}), respectively (Figure 3A). Thus, in rearing *An. campestris*-like Form E and other sibling species members of *An. barbirostris* complex in our laboratory, this method has been used routinely up until now.

1.6 Rearing condition for chromosome preparation

The results of comparison between rearing condition for a high yield of chromosomes by using 10 larvae per tray and routine rearing conditions by using 80 larvae per tray indicated that the former yielded higher percent outcomes than the latter in all experiments, *i.e.*, metaphase chromosomes-experiment I: 10 larvae (87.50%)/80 larvae (33.33%), experiment II: 10 larvae (75.00%)/80 larvae (30.00%), experiment III: 10 larvae (77.78%)/80 larvae (30.00%); salivary gland polytene chromosomes-experiment I: 10 larvae (80.00%)/80 larvae (50.00%), experiment II: 10 larvae (66.67%)/80 larvae (50.00%), experiment III: 10 larvae (100.00%)/80 larvae (66.67%).

2. Metaphase karyotype characters

A total of seventy-one isolines of *An. campestris*-like Form B, E and F from Chiang Mai, Kamphaeng Phet, Ayuttaya, Udon Thani, Khon Kaen, Mukdahan, Maha Sarakham, Chaiyaphum, Sa Kaeo, Chanthaburi, Prachuap Khiri Khan and Chumphon provinces, derived from both human-biting and animal-biting female mosquitoes, were established in the insectary. Cytological observation of F_1- and/or F_2-progenies of the 71 isolines demonstrated three forms of metaphase karyotypes, *i.e.*, Form B (X_2, Y_2), E (X_1, X_2, X_3,Y_5) and F (X_2, X_3, Y_6) (Figure 4). Form B was found in three isolines from Chiang Mai (human biting: HCmB18, HCmB20) and Kamphaeng Phet (animal biting: AKpB1); Form E was obtained in thirty-nine isolines from Chiang Mai (human biting: HCmE12, HCmE14, HCmE15), Kamphaeng Phet (human biting: HKpE1), Ayuttaya (AAyE7, AAyE8, AAyE9), Udon Thani (animal biting: AUdE2, AUdE6), Khon Kaen (animal biting: AKkE4, AKkE5, AKkE8), Mukdahan (animal biting: AMkE1, AMkE2), Maha Sarakham (animal biting: AMsE1, AMsE2, AMsE3, AMsE4, AMsE5), Sa Kaeo (human biting: HSkE2, HSkE3, HSkE4, HSkE9, HSkE10, HSkE15, HSkE17), Chanthaburi (human biting: HCtE1, HCtE2, HCtE7, HCtE14, HCtE17, HCtE18, HCtE19, HCtE20, HCtE21), Prachuap Khiri Khan (animal biting: APkE2), and Chumphon (animal biting: ACpE1, ACpE5, ACpE6); and Form F was recovered in twenty-nine isolines from Udon Thani (animal biting: AUdF3, AUdF4, AUdF5), Khon Kaen (animal biting: AKkF1, AKkF2, AKkF3, AKkF7, AKkF9), Chaiyaphum (animal biting: ACiF1), Ayuttaya (animal biting: AAyF2, AAyF3, AAyF5, AAyF6), Sa Kaeo (human biting: HSkF1, HSkF12), Chanthaburi (human biting: HCtF3, HCtF4, HCtF6, HCtF8, HCtF9, HCtF10, HCtF11, HCtF12, HCtF13,

HCtF16), Prachuap Khiri Khan (animal biting: APkF1, APkF3, APkF4), and Chumphon (animal biting: ACpF2).

In consideration of new karyotypic forms, X_2, X_3, Y_6 sex chromosomes were exhibited. The X_2 and X_3 chromosome had a submetacentric shape resembling that of the sex chromosomes of *An. barbirostris* Form A, B, C and D. The Y_6 chromosome had a large subtelocentric (acrocentric) with a considerable portion of heterochromatin present in the short arm, and it was similar in size to the X_2 chromosome. The Y_6 chromosome was quite different from Y_1 (subtelocentric/acrocentric), Y_2 (submetacentric), Y_3 (large submetacentric/metacentric) and Y_4 (medium metacentric) chromosomes of *An. barbirostris* Form A, B, C and D, respectively, and the Y (telocentric) chromosome of *An. campestris* and Y_5 (small metacentric) chromosome of *An. campestris*-like Form E. Thus, the X_2, X_3, Y_6 sex chromosomes represent a new karyotype, tentatively designated as Form F (Figure 4).

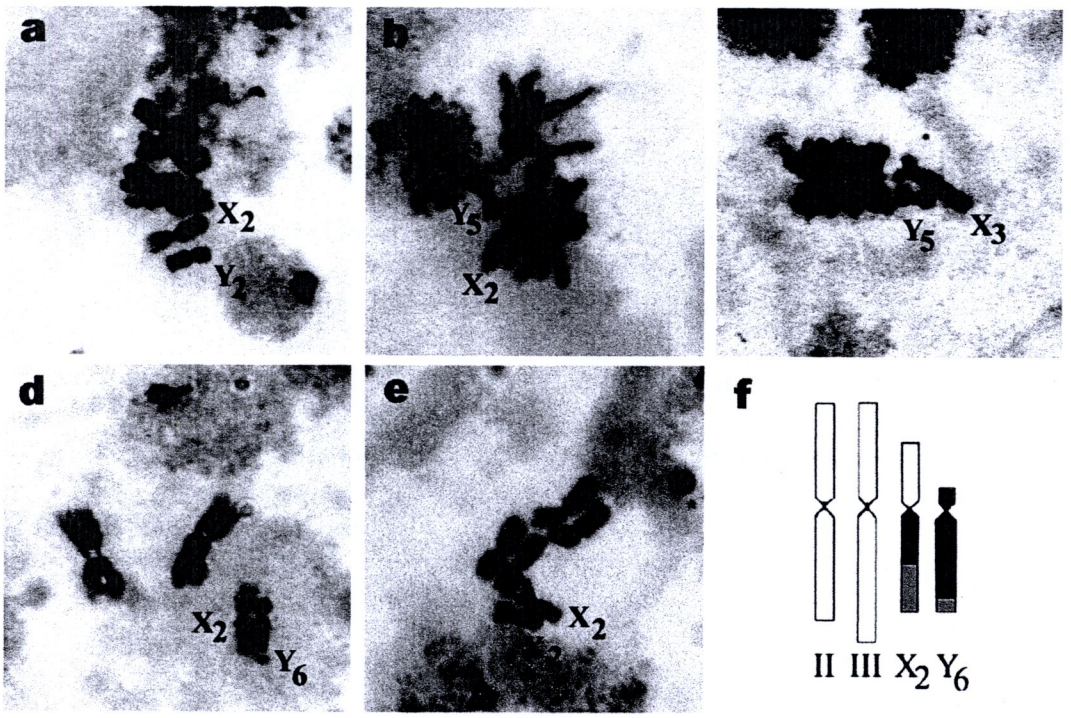

Figure 4 Metaphase karyotypes of *An. campestris*-like Form B, E and F (**a-e**). Form B: **a** Kamphaeng Phet strain, showing X_2, Y_2 chromosomes; Form E: **b** Chumphon strain, showing X_2, Y_5 chromosomes; **c** Sa Kaeo strain, showing X_3, Y_5 chromosomes; Form F: **d** Udon Thani strain, showing X_2, Y_6 chromosomes; **e** showing homozygous X_2, X_2 chromosomes; **f** Diagrams of representative metaphase karyotypes of *An. campestris*-like Form F.

3. Crossing study

Details of hatchability, pupation and emergence of parental, reciprocal and F_1-hybrid crosses among twelve isoline strains of *An. campestris*-like Form B, E and F are displayed in Table 4. Observation on the hatchability, pupation, emergence, and adult sex-ratio of parental, reciprocal and F_1-hybrid crosses revealed that all crosses yielded viable progenies, and no evidence of genetic incompatibility and/or post-mating reproductive isolation was observed among twelve isoline strains of *An. campestris*-like Form B, E and F.

Table 4 Crossing experiments among the 12 isolines of *An. campestris*-like Form B, E and F.

Crosses (Female x Male)	Total eggs (number)*	Embryonation rate**	Number hatched (%)	Number pupation (%)	Number emergence (%)	Number from total emergence (%)	
						Female	Male
Parental cross							
HCE6 x HCE6	536 (60, 476)	88	456 (85.07)	357 (78.29)	336 (94.12)	162 (48.21)	174 (51.79)
AKpB1 x AKpB1	577 (286, 291)	85	433 (75.04)	312 (72.06)	303 (97.12)	154 (50.83)	149 (49.17)
AAyF2 x AAyF2	484 (186, 298)	71	335 (69.21)	256 (76.42)	242 (94.53)	142 (58.68)	100 (41.32)
AUdF5 x AUdF5	509 (145, 364)	89	387 (76.03)	348 (89.92)	306 (87.93)	156 (50.98)	150 (49.02)
AKkE4 x AKkE4	499 (171, 328)	95	455 (91.18)	400 (87.91)	320 (80.00)	164 (51.25)	156 (48.75)
AMkE1 x AMkE1	515 (202, 313)	84	443 (86.02)	363 (81.94)	316 (87.05)	143 (45.25)	173 (54.75)
AMsE3 x AMsE3	469 (186, 283)	75	352 (75.05)	299 (84.94)	250 (83.61)	110 (44.00)	140 (56.00)
ACiF1 x ACiF1	490 (231, 259)	86	397 (81.02)	381 (95.97)	355 (93.18)	153 (43.10)	202 (56.90)
HSkE3 x HSkE3	564 (263, 301)	87	474 (84.04)	431 (90.93)	328 (76.10)	180 (54.88)	148 (45.12)
HCtF4 x HCtF4	494 (226, 268)	82	346 (70.04)	327 (94.51)	278 (85.02)	131 (47.12)	147 (52.88)
APkF1 x APkF1	525 (197, 328)	93	389 (74.10)	319 (82.01)	290 (90.91)	130 (44.83)	160 (55.17)
ACpE6 x ACpE6	566 (272, 294)	94	521 (92.05)	454 (87.14)	427 (94.05)	217 (50.82)	210 (49.18)

Table 4 (continued).

Crosses (Female x Male)	Total eggs (number)*	Embryonation rate**	Number hatched (%)	Number pupation (%)	Number emergence (%)	Number from total emergence (%)	
						Female	Male
Reciprocal cross							
HCE6 x AKpB1	473 (102, 371)	93	359 (75.90)	280 (77.99)	258 (92.14)	130 (50.39)	128 (49.61)
AKpB1 x HCE6	360 (87, 273)	74	220 (61.11)	216 (98.18)	190 (87.96)	96 (50.53)	94 (49.47)
HCE6 x AAyF2	467 (170, 297)	71	309 (66.17)	263 (85.11)	232 (88.21)	112 (48.28)	120 (51.72)
AAyF2 x HCE6	423 (207, 216)	92	360 (85.11)	266 (73.89)	218 (81.95)	97 (44.50)	121 (55.50)
HCE6 x AUdF5	398 (196, 202)	83	330 (82.91)	268 (81.21)	254 (94.78)	130 (51.18)	124 (48.82)
AUdF5 x HCE6	485 (184, 301)	96	378 (77.94)	318 (84.13)	309 (97.17)	151 (48.87)	158 (51.13)
HCE6 x AKkE4	402 (171, 231)	94	382 (95.02)	330 (86.39)	307 (93.03)	169 (55.05)	138 (45.95)
AKkE4 x HCE6	306 (119, 187)	62	189 (61.76)	136 (71.96)	117 (86.03)	63 (53.85)	54 (46.15)
HCE6 x AMkE1	499 (186, 313)	95	459 (91.98)	418 (91.07)	372 (89.00)	179 (48.12)	193 (51.88)
AMkE1 x HCE6	424 (138, 286)	86	344 (81.13)	337 (97.97)	317 (94.07)	139 (43.85)	178 (56.15)
HCE6 x AMsE3	440 (193, 247)	81	339 (77.05)	281 (82.89)	235 (83.63)	120 (51.06)	115 (48.94)
AMsE3 x HCE6	409 (180, 229)	90	295 (72.13)	233 (78.98)	192 (82.40)	102 (53.12)	90 (46.88)

Table 4 (continued).

Crosses (Female x Male)	Total eggs (number)*	Embryonation rate**	Number hatched (%)	Number pupation (%)	Number emergence (%)	Number from total emergence (%)	
						Female	Male
Reciprocal cross							
HCE6 x ACiF1	431 (211, 220)	91	375 (87.01)	357 (95.20)	332 (93.00)	149 (44.88)	183 (55.12)
ACiF1 x HCE6	378 (118, 260)	98	352 (93.12)	334 (94.89)	301 (90.12)	166 (55.15)	135 (44.85)
HCE6 x HSkE3	357 (161, 196)	82	253 (70.87)	238 (94.07)	196 (82.35)	84 (42.86)	112 (57.14)
HSkE3 x HCE6	408 (145, 263)	76	249 (61.03)	243 (97.59)	224 (92.18)	125 (55.80)	99 (44.20)
HCE6 x HCtF4	346 (147, 199)	84	287 (82.95)	241 (83.97)	201 (83.40)	87 (43.28)	114 (56.72)
HCtF4 x HCE6	436 (138, 298)	91	388 (88.99)	380 (97.94)	365 (96.05)	186 (50.96)	179 (49.04)
HCE6 x APkF1	472 (212, 260)	94	402 (85.17)	370 (92.04)	300 (81.08)	135 (45.00)	165 (55.00)
APkF1 x HCE6	403 (172, 231)	89	283 (70.22)	253 (89.40)	235 (92.89)	133 (56.60)	102 (43.40)
HCE6 x ACpE6	383 (33, 350)	90	306 (79.90)	301 (98.37)	247 (82.06)	114 (46.15)	133 (53.85)
ACpE6 x HCE6	473 (159, 314)	99	445 (94.08)	414 (93.03)	385 (93.00)	177 (45.97)	208 (54.03)

Table 4 (continued).

Crosses (Female x Male)	Total eggs (number)*	Embryonation rate**	Number hatched (%)	Number pupation (%)	Number emergence (%)	Number from total emergence (%)	
						Female	Male
F_1 cross							
(HCE6 x AKpB1)F_1 x (HCE6 x AKpB1)F_1	407 (180, 227)	90	366 (89.93)	278 (75.96)	231 (83.09)	137 (59.31)	94 (40.69)
(AKpB1 x HCE6)F_1 x (AKpB1 x HCE6)F_1	399 (75, 324)	91	303 (75.94)	251 (82.84)	226 (90.04)	104 (46.02)	122 (53.98)
(HCE6 x AAyF2)F_1 x (HCE6 x AAyF2)F_1	529 (226, 303)	81	397 (75.05)	369 (92.95)	317 (85.91)	158 (49.84)	159 (50.16)
(AAyF2 x HCE6)F_1 x (AAyF2 x HCE6)F_1	541 (224, 317)	86	422 (78.00)	301 (71.33)	265 (88.04)	135 (50.94)	130 (49.06)
(HCE6 x AUdF5)F_1 x (HCE6 x AUdF5)F_1	485 (157, 328)	87	407 (83.92)	338 (83.05)	294 (86.98)	141 (47.96)	153 (52.04)
(AUdF5 x HCE6)F_1 x (AUdF5 x HCE6)F_1	438 (159, 279)	81	350 (79.91)	317 (90.57)	282 (88.96)	127 (45.04)	155 (54.96)
(HCE6 x AKkE4)F_1 x (HCE6 x AKkE4)F_1	459 (225, 234)	73	317 (69.06)	288 (90.85)	265 (92.01)	138 (52.08)	127 (47.92)
(AKkE4 x HCE6)F_1 x (AKkE4 x HCE6)F_1	400 (136, 264)	77	280 (70.00)	262 (93.57)	215 (82.06)	109 (50.70)	106 (49.30)
(HCE6 x AMkE1)F_1 x (HCE6 x AMkE1)F_1	420 (116, 304)	96	386 (91.90)	317 (82.12)	247 (77.92)	101 (40.89)	146 (59.11)
(AMkE1 x HCE6)F_1 x (AMkE1 x HCE6)F_1	489 (204, 285)	97	449 (91.82)	332 (73.94)	252 (75.90)	128 (50.79)	124 (49.21)
(HCE6 x AMsE3)F_1 x (HCE6 x AMsE3)F_1	439 (77, 362)	91	356 (81.09)	263 (73.88)	228 (86.69)	120 (52.63)	108 (47.37)
(AMsE3 x HCE6)F_1 x (AMsE3 x HCE6)F_1	507 (211, 296)	93	451 (88.95)	343 (76.05)	281 (81.92)	129 (45.91)	152 (54.09)

Table 4 (continued).

Crosses (Female x Male)	Total eggs (number)*	Embryonation rate**	Number hatched (%)	Number pupation (%)	Number emergence (%)	Number from total emergence (%)	
						Female	Male
(HCE6 x ACiF1)F_1 x (HCE6 x ACiF1)F_1	493 (221, 272)	90	434 (88.03)	352 (81.11)	250 (71.02)	132 (52.80)	118 (47.20)
(ACiF1 x HCE6)F_1 x (ACiF1 x HCE6)F_1	491 (201, 290)	79	349 (71.08)	293 (83.95)	252 (86.01)	116 (46.03)	136 (53.97)
(HCE6 x HSkE3)F_1 x (HCE6 x HSkE3)F_1	443 (154, 289)	89	381 (86.00)	312 (81.89)	275 (88.14)	140 (50.91)	135 (49.09)
(HSkE3 x HCE6)F_1 x (HSkE3 x HCE6)F_1	531 (249, 282)	98	494 (93.03)	449 (90.89)	350 (77.95)	161 (46.00)	189 (54.00)
(HCE6 x HCtF4)F_1 x (HCE6 x HCtF4)F_1	374 (101, 273)	93	359 (95.99)	330 (91.92)	271 (81.12)	146 (53.87)	125 (46.13)
(HCtF4 x HCE6)F_1 x (HCtF4 x HCE6)F_1	424 (79, 345)	86	399 (94.10)	391 (97.99)	305 (78.01)	135 (44.26)	170 (55.74)
(HCE6 x APkF1)F_1 x (HCE6 x APkF1)F_1	506 (227, 279)	80	380 (75.10)	331 (87.11)	245 (74.02)	118 (48.16)	127 (51.84)
(APkF1 x HCE6)F_1 x (APkF1 x HCE6)F_1	531 (259, 272)	92	431 (81.17)	344 (79.81)	276 (80.23)	141 (51.09)	135 (48.91)
(HCE6 x ACpE6)F_1 x (HCE6 x ACpE6)F_1	545 (269, 276)	91	447 (82.02)	387 (86.58)	325 (83.98)	136 (41.85)	189 (58.15)
(ACpE6 x HCE6)F_1 x (ACpE6 x HCE6)F_1	397 (69, 328)	89	346 (87.15)	243 (70.23)	224 (92.18)	106 (47.32)	118 (52.68)

* Two selective egg-batches of inseminated females from each cross; ** Dissection from 100 eggs.

4. DNA sequences and phylogenetic analysis

DNA sequences were determined and analyzed for the ITS2, COI, and COII regions of the twenty-eight isolines of *An. campestris*-like Form B, E and F from twelve provinces in Thailand (Table 5). All isolines showed the same length for the ITS2 (1,651 bp), COI (658 bp) and COII (685 bp). Each species of *An. barbirostris* A1, A2, A3, A4 and *An. campestris*-like had different length for the ITS2 region (Saeung *et al*, 2007; 2008; Suwannamit *et al*, 2009). All isolines from the present study, including the new karyotypic form, had the same length for the ITS2 region as that of *An. campestris*-like in the previous studies. To reveal the evolutionary relationship among the three karyotypic forms of *An. campestris*-like, neighbor-joining trees were made (Figure 5-7). The trees for ITS2, COI and COII separated twenty-eight isolines of *An. campestris*-like Form B, E and F from the other species, with strongly supported bootstrap probabilities (98-100%). But, in the clade of *An. campestris*-like of the trees, the isolines of Form B, E, and F were nested. Additionally, averages genetic distances within and between the karyotypic forms were listed in Table 6, indicating low intraspecific variation (0.001-0.004) both within and between the forms for the three regions.

Table 5 Locations, isoline colonies and karyotypic forms of *An. campestris*–like and their GenBank accession numbers.

Location	Code of isoline*	Karyotypic form	Length of ITS2 (bp)	Region	Genbank accession number		
					ITS2	COI	COII
Chiang Mai							
	HCE6**	E	1,651	ITS2, COI, COII	AB331566	AB331583	AB331604
	HCB9	B	1,651	ITS2, COI, COII	AB331563	AB331582	AB331601
	HCmE12	E	1,651	ITS2, COI, COII	AB436074	AB436102	AB436130
	HCmE14	E	1,651	ITS2, COI, COII	AB436075	AB436103	AB436131
	HCmE15	E	1,651	ITS2, COI, COII	AB436076	AB436104	AB436132
	HCmB18	B	1,651	ITS2, COI, COII	AB436077	AB436105	AB436133
	HCmB20	B	1,651	ITS2, COI, COII	AB436078	AB436106	AB436134
Kamphaeng Phet	AKpB1**	B	1,651	ITS2, COI, COII	AB436079	AB436107	AB436135
	HKpE1	E	1,651	ITS2, COI, COII	AB436080	AB436108	AB436136
Ayuttaya	AAyF2**	F	1,651	ITS2, COI, COII	AB436081	AB436109	AB436137
	AAyF6	F	1,651	ITS2, COI, COII	AB436082	AB436110	AB436138
	AAyE7	E	1,651	ITS2, COI, COII	AB436083	AB436111	AB436139

Table 5 (continued).

Location	Code of isoline*	Karyotypic form	Length of ITS2 (bp)	Region	Genbank accession number		
					ITS2	COI	COII
Udon Thani	AUdF3	F	1,651	ITS2, COI, COII	AB436084	AB436112	AB436140
	AUdF4	F	1,651	ITS2, COI, COII	AB436085	AB436113	AB436141
	AUdF5**	F	1,651	ITS2, COI, COII	AB436086	AB436114	AB436142
Khon Kaen	AKkF1	F	1,651	ITS2, COI, COII	AB436087	AB436115	AB436143
	AKkE4**	E	1,651	ITS2, COI, COII	AB436088	AB436116	AB436144
	AKkE8	E	1,651	ITS2, COI, COII	AB436089	AB436117	AB436145
Maha Sarakham	AMsE3**	E	1,651	ITS2, COI, COII	AB436090	AB436118	AB436146
	AMsE4	E	1,651	ITS2, COI, COII	AB436091	AB436119	AB436147
	AMsE5	E	1,651	ITS2, COI, COII	AB436092	AB436120	AB436148
Mukdahan	AMkE1**	E	1,651	ITS2, COI, COII	AB436093	AB436121	AB436149
Chaiyaphum	ACiF1**	F	1,651	ITS2, COI, COII	AB436094	AB436122	AB436150
Sa Kaeo	HSkF1	F	1,651	ITS2, COI, COII	AB436095	AB436123	AB436151
	HSkE2	E	1,651	ITS2, COI, COII	AB436096	AB436124	AB436152
	HSkE3**	E	1,651	ITS2, COI, COII	AB436097	AB436125	AB436153

Table 5 (continued).

Location	Code of isoline*	Karyotypic form	Length of ITS2 (bp)	Region	Genbank accession number		
					ITS2	COI	COII
Chanthaburi	HCtE2	E	1,651	ITS2, COI, COII	AB436098	AB436126	AB436154
	HCtF4**	F	1,651	ITS2, COI, COII	AB436099	AB436127	AB436155
Prachuap Khiri Khan	APkF1**	F	1,651	ITS2, COI, COII	AB436100	AB436128	AB436156
Chumphon	ACpE6**	E	1,651	ITS2, COI, COII	AB436101	AB436129	AB436157

*: H-human bait, A-animal bait; **: Isolines used in crossing experiments.

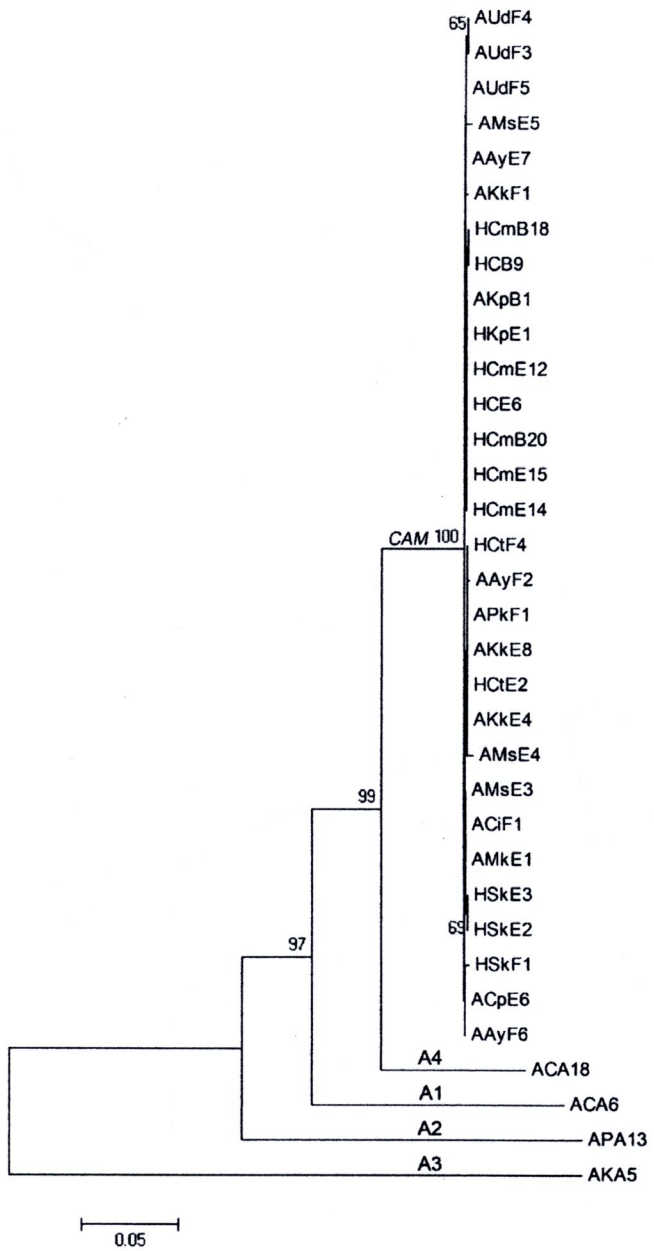

Figure 5 A phylogenetic trees of *An. campestris*-like Form B, E and F (*CAM*) based on molecular analysis of ITS2. The tree was generated by neighbor-joining analysis. Numbers on the nodes indicate probabilities based on 1,000 bootstrap replicates. A probability of more than 50% is shown. Branch lengths are proportional to genetic distance (scale bar).

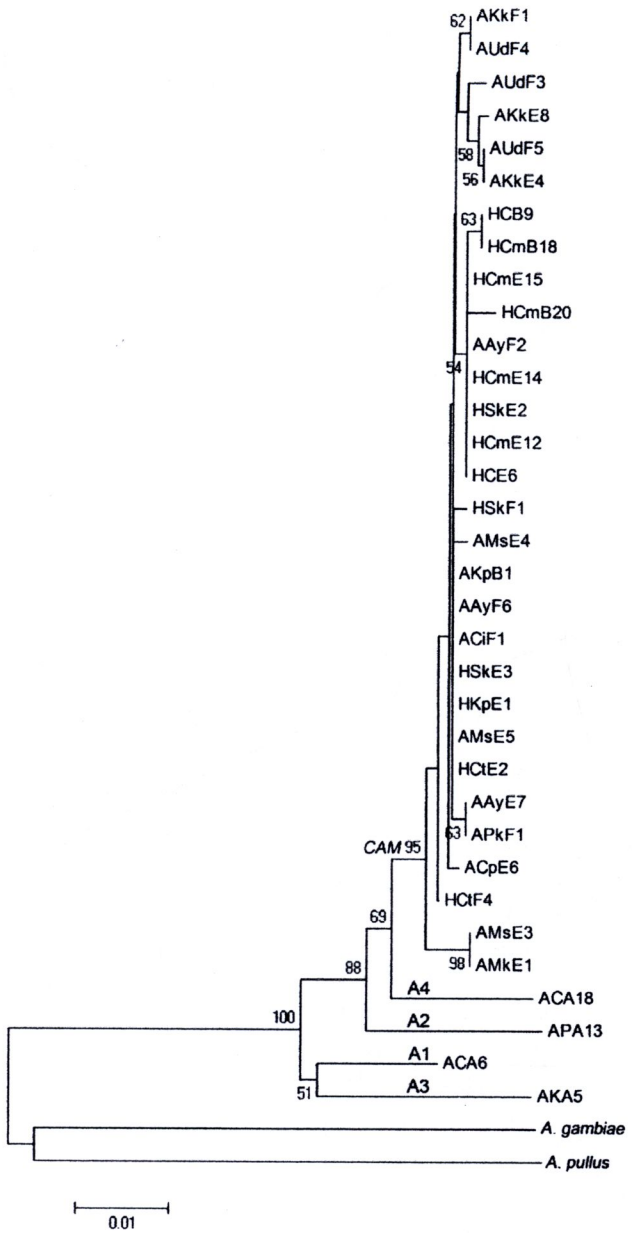

Figure 6 A phylogenetic trees of *An. campestris*-like Form B, E and F (*CAM*) based on molecular analysis of COI. The tree was generated by neighbor-joining analysis. Numbers on the nodes indicate probabilities based on 1,000 bootstrap replicates. A probability of more than 50% is shown. Branch lengths are proportional to genetic distance (scale bar).

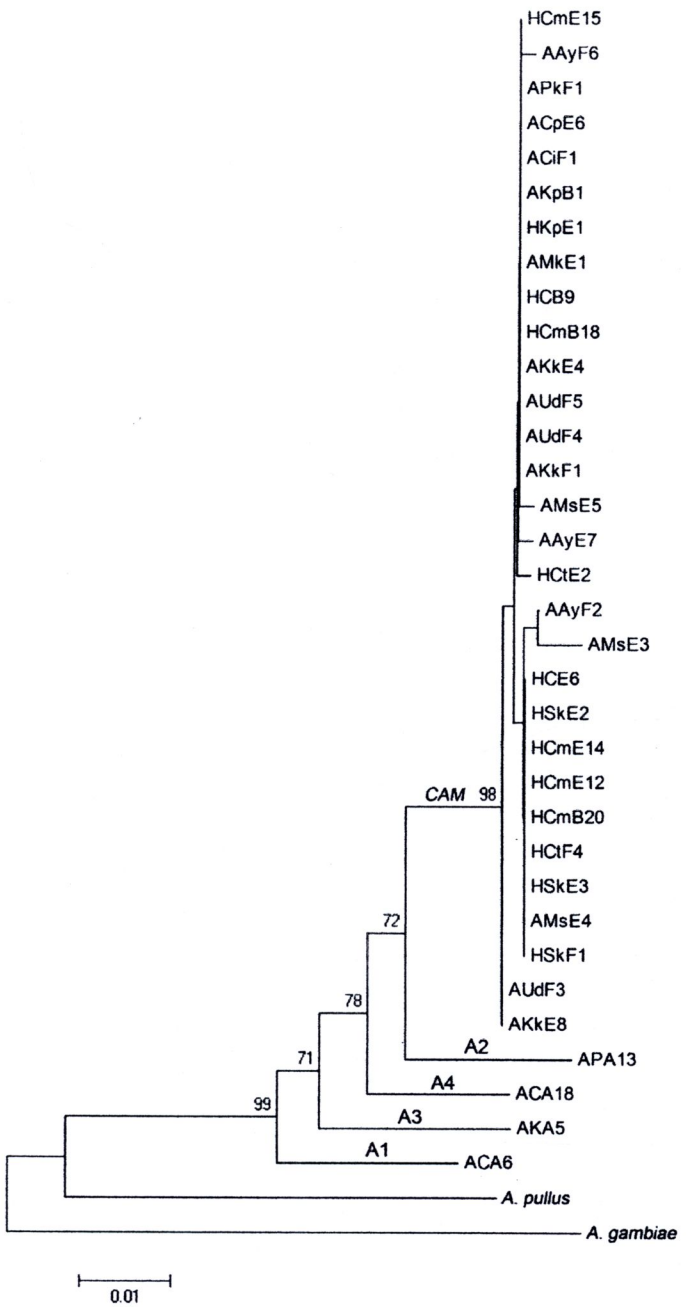

Figure 7 A phylogenetic tree of *An. campestris*-like Form B, E and F (*CAM*) based on molecular analysis of COII. The tree was generated by neighbor-joining analysis. Numbers on the nodes indicate probabilities based on 1,000 bootstrap replicates. A probability of more than 50% is shown. Branch lengths are proportional to genetic distance (scale bar).

Table 6 Average genetic distance within and between the *An. campestris*-like Form B, E and F for the ITS2, COI and COII regions.

	ITS2	COI	COII
Within Form			
B	0.001	0.004	0.001
E	0.002	0.004	0.002
F	0.002	0.003	0.002
Between Forms			
B-E	0.002	0.004	0.001
B-F	0.002	0.004	0.001
E-F	0.002	0.003	0.002

5. Morphological studies of eggs, larvae, pupae and adults under light microscope

The characteristics for morphological investigations of eggs, larvae, pupae and adults were depending upon the standard description of Reid (1968), and Harrison and Scanlon (1975). A total of 71 material samples of eggs, larvae, pupae and adults of F_1- and/or F_2-progeny derived from 71 isolines were used for examination. Comparative morphology of larvae, *i.e.*, summation of branches of seta 5-I (6-9), 5-III (11-17) and 5-VII (8-16), and seta 13-I (14-31), 13-II (17-25), 13-III (13-24) and 13-IV (8-14); and pupae, *i.e.*, seta 2-III (10-19), 2-VI (20.3-30.0 branches), and 2-VII (10-18); and adults, *i.e.*, color of wing (light- and dark-winged type), pale sterna scales, and hind tarsal pale band, the results of examination revealed that all characteristics were cryptic differentiation among *An. campestris*-like strains and/or karyotypic forms.

6. Morphological studies of eggs under scanning electron microscopy

The morphological feature and exochorionic sculpturing of *An. campestris*-like Form B, E and F was generally similar (Figure 8, 9), and no account of species specific characteristics that could be used to differentiate and/or characterize under SEM. The eggs were boat-shaped, with a somewhat broader anterior or head-end (Figure 8A). Viewed laterally, the contour of the entire egg was concave on the morphologically dorsal surface and convex on the ventral surface (Figure 8B). The middle region of each egg side was dominated by a float with approximately 31 ribs. Viewed dorsally, there was a bare area, which was surrounded by the two longitudinal bands of a sclerotized ridge-like frill; this bare area is called the deck. The deck was continuous for the whole length of the egg and slightly constricted near the midline

(Figure 8A). At each end of the egg on the dorsal surface were large-lobed tubercles that ranged from 4-5 in number. Large-lobed tubercles on the anterior and posterior ends were rosette-shaped, giving rise to 6-7 lateral lobes, and surrounded by a sclerotized ridge and raised border (Figure 8C). The tubercles on the deck were irregularly jagged and surrounded by other much smaller, irregular tubercles (Figure 8D). The inner surface of the frill was of a sclerotized, ridged-like texture and marked by picket like-ribs (Figure 9A); the outer surface was smooth with a parallel brick-like texture along its entire length (Figure 9B). The exochorionic sculpturing appears as more or less regularly hexagonal reticulum. The reticulum is found throughout the entire egg except at the deck. It is formed by membrane like-wall enclosing many small, less prominent tubercles (Figure 9C). Downward to the anterior end, the micropylar orifice could be seen clearly. It was surrounded by a smooth collar that had an irregular outer margin about 6 spurs that extended radially toward the central orifice (Figure 9D).

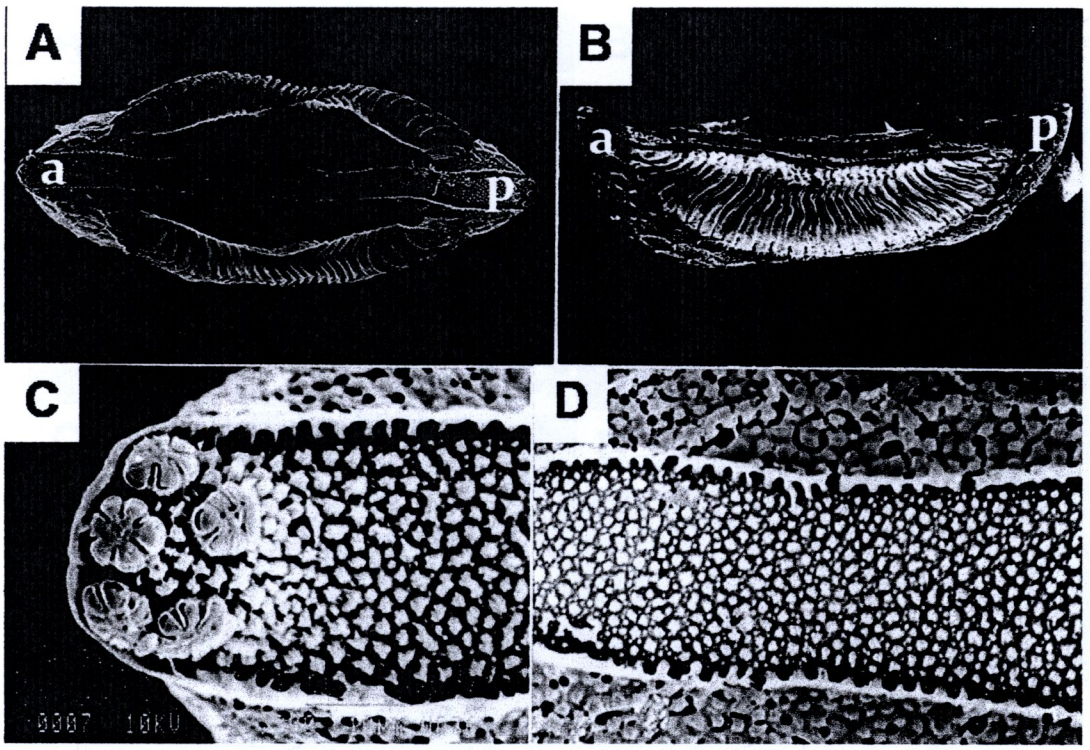

Figure 8 Egg surface topography of *An. campestris*-like under scanning electron microscope (SEM); whole eggs: (A) dorsal aspect, anterior end (a), posterior end (p) (x 230). (B) Lateral aspect, anterior end (a), posterior end (p) (x 250). (C) Anterior end, showing irregularly jagged tubercles on the deck and four large, rosette-shaped tubercles (2,200). (D) A higher magnification of the irregularly jagged tubercles on the deck (x 7,000).

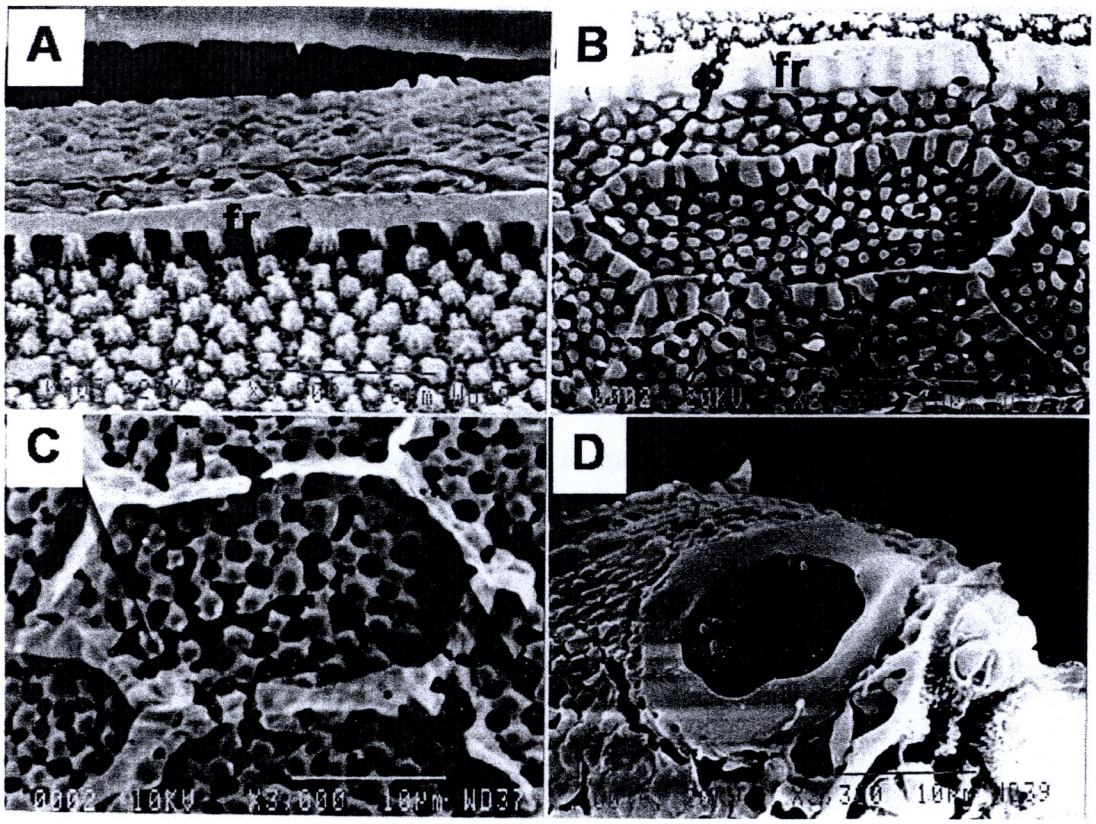

Figure 9 Egg surface topography of *An. campestris*-like under scanning electron microscope (SEM): (A) the inner surface of the frill (fr), showing its sclerotized, ridge-like texture with picket-like ribs (x 3,500). (B) The outer surface of the frill (fr), showing its smooth surface and parallel brick-like texture along its entire length (x 3,500). (C) The exochorionic sculptering in the middle of the egg, showing more or less regularly hexagonal reticulum with membrane like-wall enclosing many small, less prominent tubercles. (D) The anterior end, showing the micropylar orifice surrounded by a smooth collar with an irregular outer margin (x 3,300).

7. Salivary gland polytene chromosome investigation

When comparing bands on the same arm of X-chromosome and autosomes (2R, 2L, 3R and 3L) among 12 strains of *An. campestris*-like Form B (Figure 10), E (Figure 11) and F (Figure 12), no major chromosomal rearrangement that related to the strains and/or karyotypic variations were demonstrated. In addition, the homosequential synapsis salivary gland polytene chromosomes of F_1-hybrid larvae from the crosses among *An. campestris*-like forms were good supportive evidence.

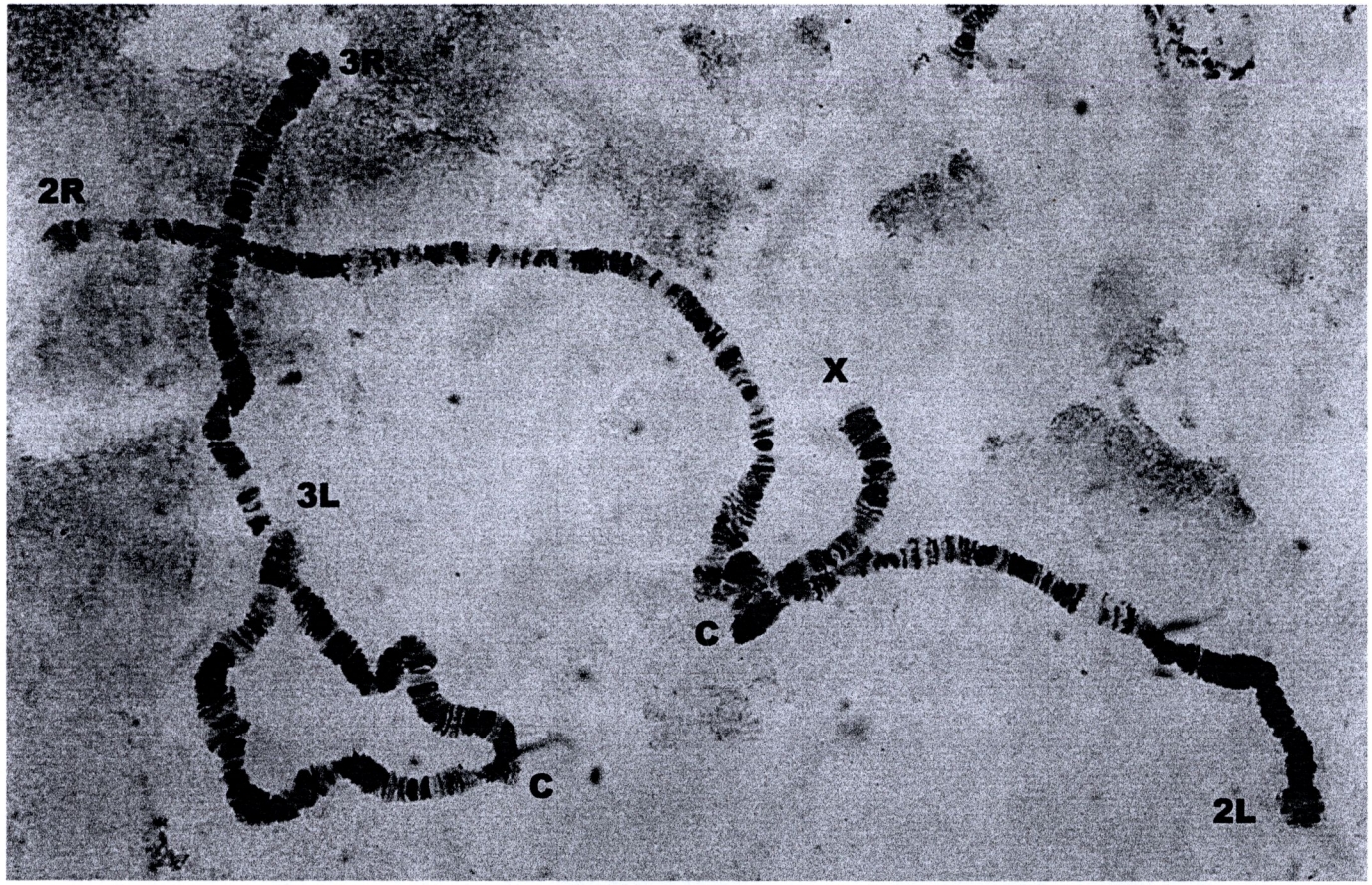

Figure 10 Complete set of salivary gland polytene chromosomes of *An. campestris*-like Form B (C = Centromere, L = Left arms, R = Right arms, X = X-chromosome).

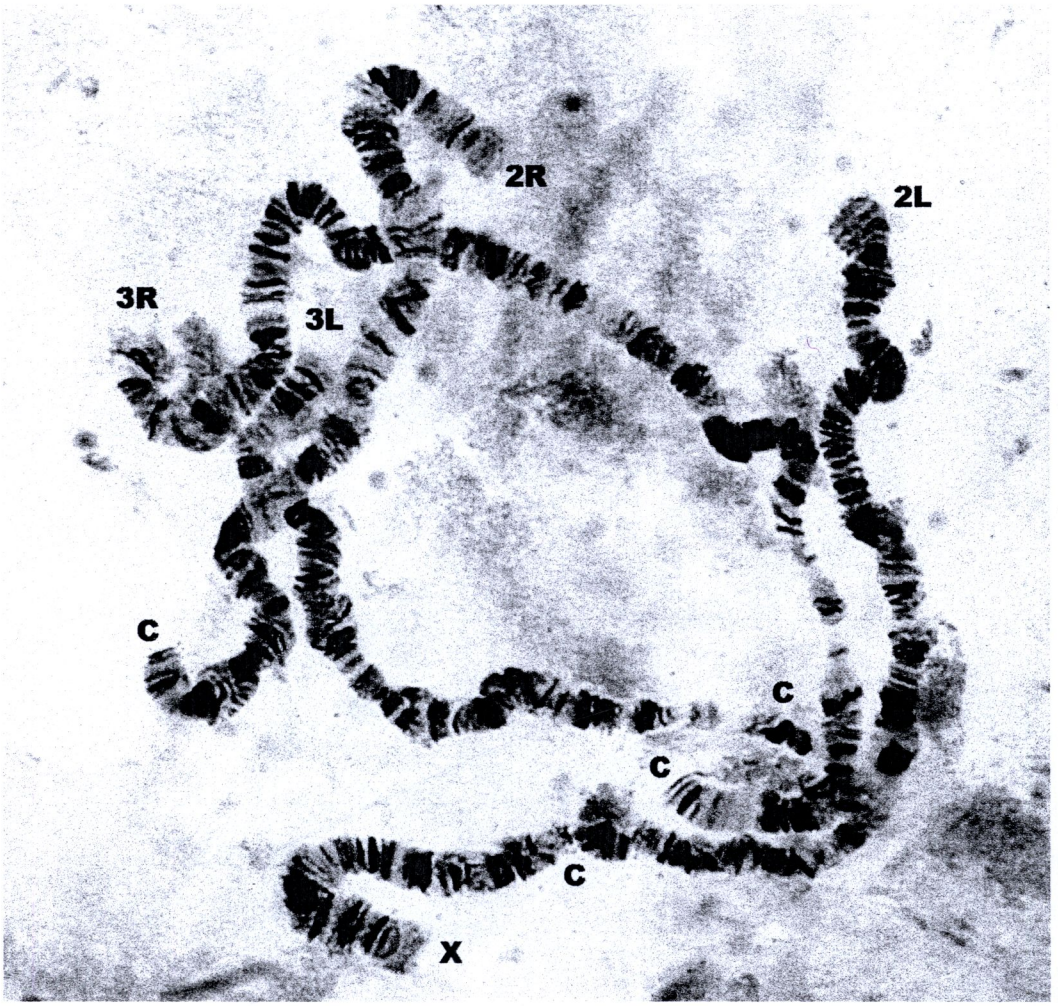

Figure 11 Complete set of salivary gland polytene chromosomes of *An. campestris*-like Form E (C = Centromere, L = Left arms, R = Right arms, X = X-chromosome).

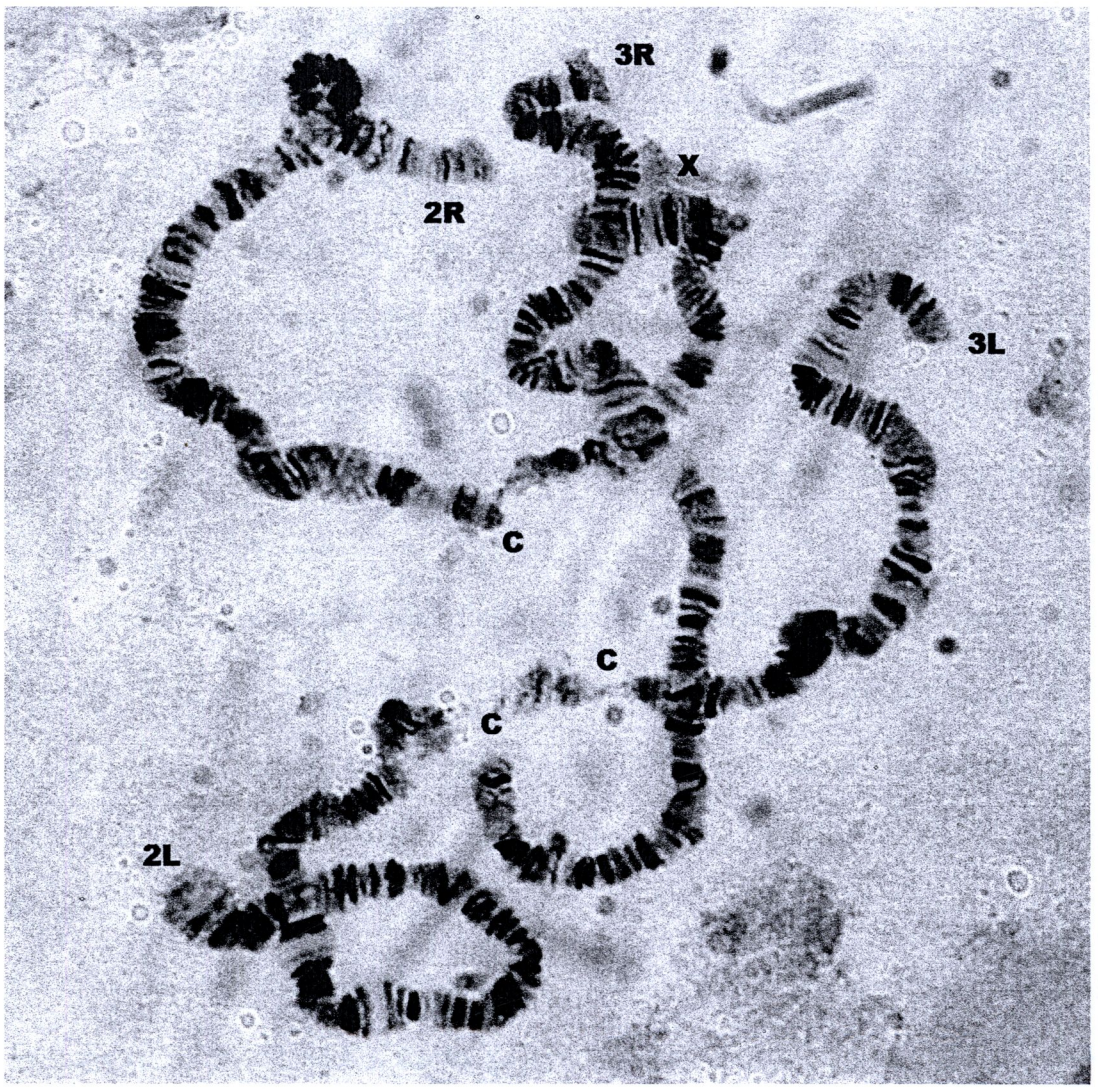

Figure 12 Complete set of salivary gland polytene chromosomes of *An. campestris*-like Form F (C = Centromere, L = Left arms, R = Right arms, X = X-chromosome).

8. Malaria susceptibility test

Details of oocyst and sporozoite rates are shown in Table 7 and 8. The 100% oocyst rate and 93.33% sporozoite rate, and 100% oocyst rate and 85.71-92.31% sporozoite rates obtained from *An. cracens* (the outgroup control mosquito-vector) from experimental feedings of blood containing gametocytes of *P. falciparum* and *P. vivax*, respectively, indicated that all feedings were conditional experiments, which reflected on the proper density and maturity of infective gametocytes in infected blood.

In the experimental feedings of *P. falciparum*, represented *An. campestris*-like Form E (Chiang Mai strain) and F (Udon Thani strain) were refractory to *P. falciparum* by providing 0% oocyst and sporozoite rate, while 100% oocyst and 93.33% sporozoite rates were obtained from the out group control mosquito-vector, *An. cracens* (Table 7).

In the experimental feedings of *P. vivax* (Table 8), comparative statistical analyses of the oocyst rates and average number of oocysts per infected midgut of *An. campestris*-like [oocyst rates: Form B (100%) and (66.67%), and E (100%) and (100%), 8 and 14 days, respectively, after feeding; average number oocyst per infected midgut: Form B (77.60) and (20.75), and E (131.00) and (42.00), 8 and 14 days, respectively, after feeding], and *An. cracens*, an efficient control-vector, exhibited no significant difference ($p > 0.05$). Likewise, the sporozoite rates of *An. campestris*-like [Form B (66.67%) and E (64.29%), 14 days after feeding], did not differ significantly from *An. cracens* ($p > 0.05$). The characteristics of oocysts in midguts and sporozoites from squashed salivary glands of *An. cracens* and *An campestris*-like Form E are shown in Figures 13 and 14, respectively.

An. campestris-like Form E (Sa Kaeo strain) and F (Ayuttaya strain): the oocyst rates of *An. campestris*-like Form E [experiment II (60%) and III (40%), 8 days after feeding; experiment II (33.33%) and III (0%), 14 days after feeding] and F [experiment II (40%) and III (20%), 8 days after feeding; experiment II (12.50%) and III (0%), 14 days after feeding], and the average number of oocysts per infected midgut of *An. campestris*-like Form E [experiment II (20.33) and III (2.50), 8 days after feeding; experiment II (12.20) and III (0), 14 days after feeding] and F [experiment II (8.50) and III (1.50), 8 days after feeding; experiment II (2.50) and III (0), 14 days after feeding], were lower than *An. cracens*, an efficient control-vector, in all experimental studies. Comparative statistical analyses of the oocyst rates and average number of oocysts per infected midgut between *An. cracens* and *An. campestris*-like Form E and F, 8 days after feeding, were performed. The results demonstrated that only the oocyst rates between *An. cracens* and *An. campestris*-like Form F (experiment III) differed significantly ($p < 0.05$), whereas only the average number of oocysts per infected midgut between *An. cracens* and *An. campestris*-like Form E and F (experiment III) did not differ significantly ($p > 0.05$). Comparative statistical analyses of the oocyst rates and average number of oocysts per infected midgut between *An. cracens* and *An. campestris*-like Form E and F, 14 day after feeding, were not done because during this period the mature oocysts from the midguts of *An. cracens* ruptured and yielded unreliable results. It was interesting to note that different stages of oocyst development could be observed in *An. campestris*-like Form E and F, when compared with *An. cracens*. Most of the oocysts recovered from *An. cracens*, 8 and 14 days after feeding, showed a mature stage of development, with a wheel-shaped pattern of sporozoites inside cysts, while in *An. campestris*-like

Form E (Sa Kaeo strain) and F (Ayuttaya strain), all of the investigated oocysts had abnormal development, with retaining stages and some forming melanin inside cysts. The sporozoite rates of *An. campestris*-like Form E and F (experiment II and III) were 0% 14 days after feedings. The results revealed that only *An. campestris*-like Form B and E strain from Chiang Mai province were proven to be the efficiently potential vector for *P. vivax*.

Table 7 Oocysts and sporozoites detected from *An. cracens* and *An. campestris*-like Form E and F 8 and 14 days post infection with *P. falciparum* (gametocyte density/200 wbc = 40).

Mosquito species	8 days		14 days		
	Oocyst rate (number)	Average number of oocysts per infected midgut (range)	Oocyst rate (number)	Average number of oocysts per infected midgut (range)	Sporozoite rate (number)
An. cracens	100 (5/5)	114.80 ± 25.26 (79-141)	86.67 (13/15)	86.38 ± 65.39 (4-201)	93.33 (14/15)
An. campestris-like forms					
E (CM)	0 (0/5)	0	0 (0/14)	0	0 (0/14)
F (UD)	0 (0/5)	0	0 (0/12)	0	0 (0/12)

CM: Chiang Mai strain; UD: Udon Thani strain

Table 8 Oocysts and sporozoites detected from *An. cracens* and *An. campestris*-like Form B, E and F 8 and 14 days post infection with *P. vivax* (gametocyte density/200wbc = 32, 15 and 20 in experiment I, II and III, respectively).

Mosquito species	8 days		14 days		
	Oocyst rate (number)	Average number of oocysts per infected midgut (range)	Oocyst rate (number)	Average number of oocysts per infected midgut (range)	Sporozoite rate (number)
Experiment I					
An. cracens	100 (5/5)	108.60 ± 38.22 (53-136)	90.00 (18/20)	48.44 ± 17.84 (17-78)	90.00 (18/20)
An. campestris-like forms					
B (CM)	100 (5/5)	77.60 ± 37.33 (29-130)	66.67 (4/6)	20.75 ± 9.91 (8-32)	66.67 (4/6)
E (CM)	100 (5/5)	131.00 ± 42.95 (91-194)	100 (14/14)	42.00 ± 14.90 (14-77)	64.29 (9/14)
Experiment II					
An. cracens	100 (5/5)	145.00 ± 93.37 (11-245)	85.71 (18/21)	40.17 ± 66.38 (1-248)	85.71 (18/21)
An. campestris-like forms					
E (SK)	60 (3/5)	20.33 ± 16.44 (8-39)**	33.33 (5/15)	12.20 ± 9.73 (3-24)	0 (0/15)
F (AY)	40 (2/5)	8.50 ± 4.95 (5-12)**	12.50 (2/16)	2.50 ± 2.12 (1-4)	0 (0/16)
Experiment III					
An. cracens	100 (5/5)	10.20 ± 6.46 (1-18)	76.92 (10/13)	4.50 ± 2.07 (1-7)	92.31 (12/13)
An. campestris-like forms					
E (SK)	40 (2/5)	2.50 ± 0.71 (2-3)	0 (0/12)	0	0 (0/12)
F (AY)	20 (1/5)*	1.50 ± 0.71 (1-2)	0 (0/14)	0	0 (0/14)

CM: Chiang Mai strain; SK: Sa Kaeo strain; AY: Ayuttaya strain; Oocyst rate: *, $p < 0.05$ (Fisher exact test); Average number of oocyst per infected midgut: **, $p < 0.05$ (t-test, two-sides); sporozoite rate.

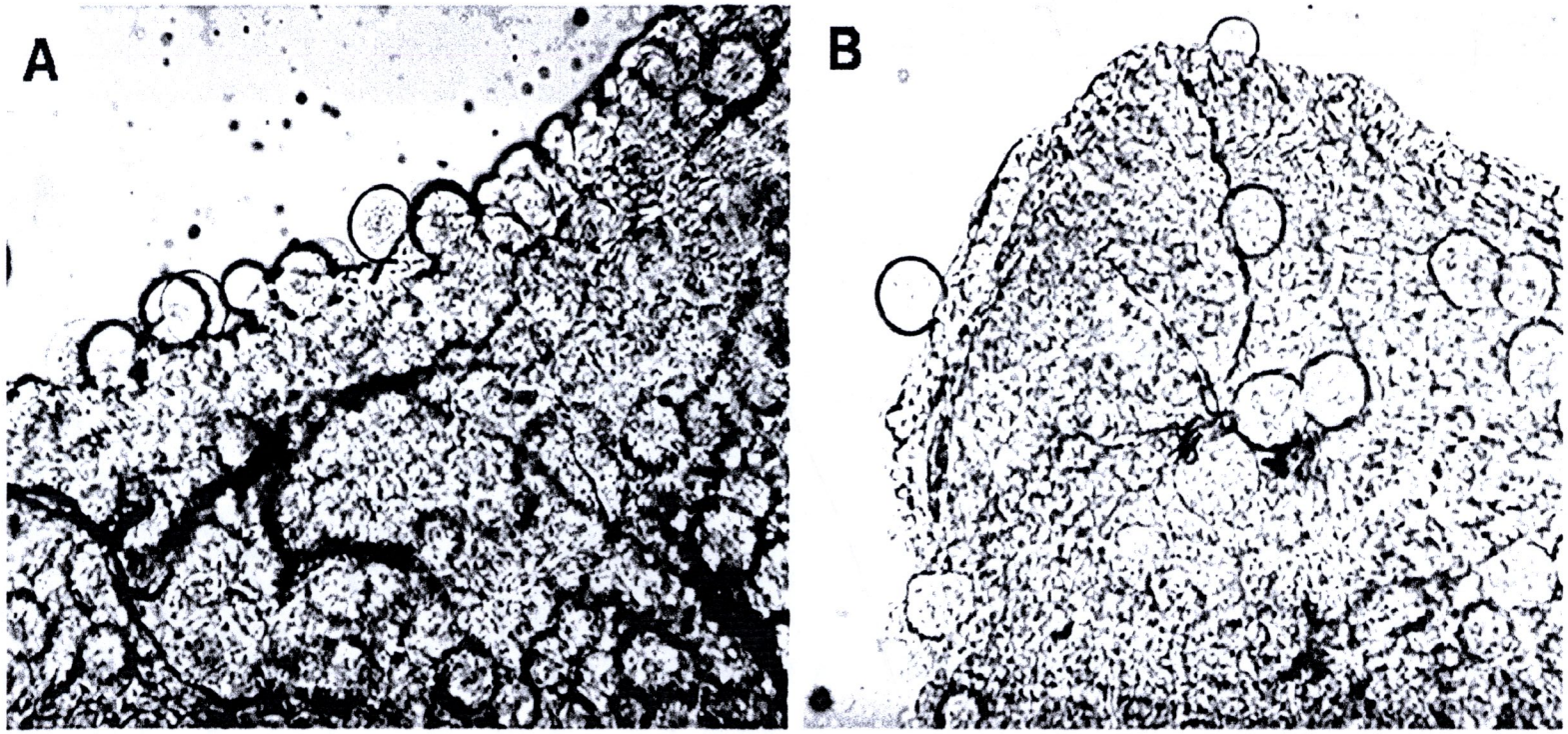

Figure 13 Oocysts of *P. vivax* recovered from midgut of (A) *An. cracens* and (B) *An. campestris*-like Form E (Chiang Mai) on day 8 after infection.

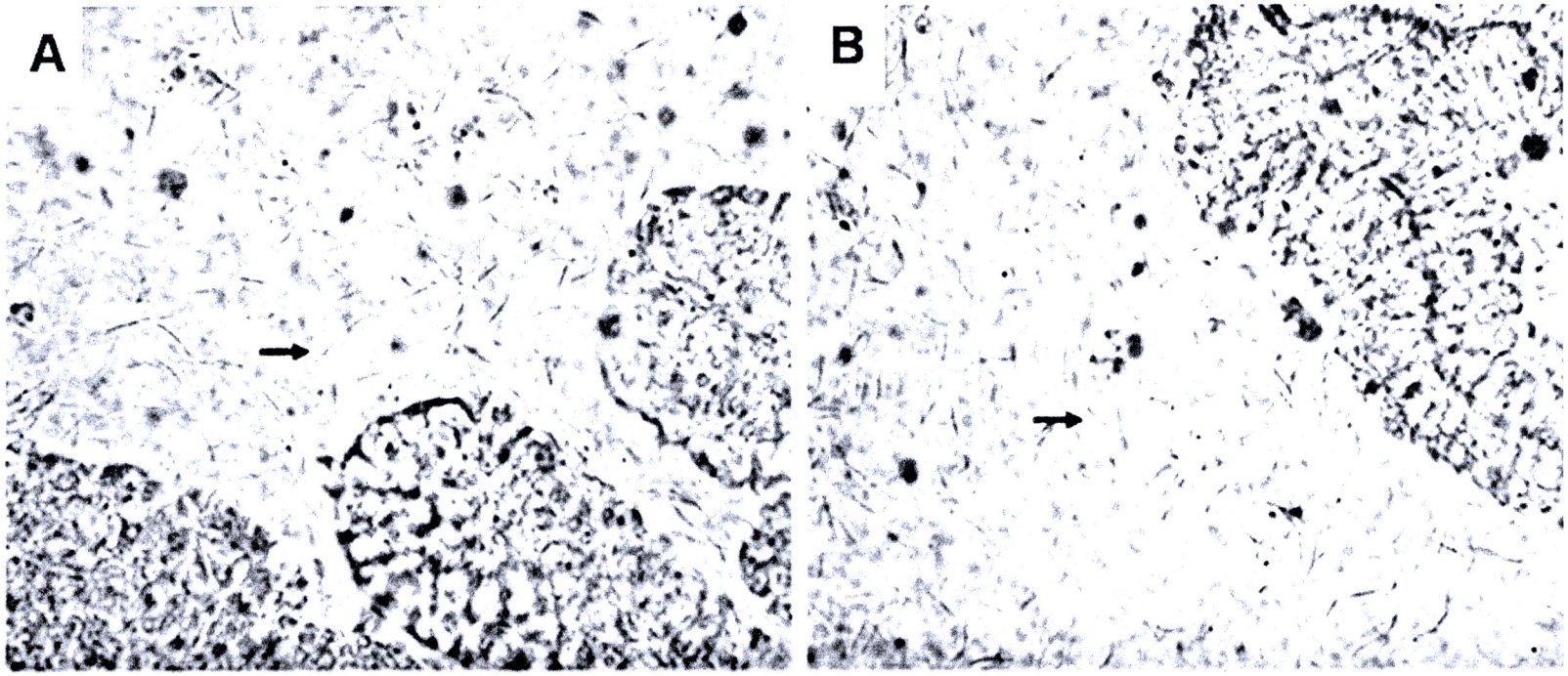

Figure 14 Free flow regular spindle-shaped sporozoites of *P. vivax* from the squashed salivary glands (small arrow) (A) *An. cracens* and (B) *An. campestris*-like Form E (Chiang Mai) on day 14 after infection.